ROYAL SOCIETY
OF CHEMISTRY

PAPER

Check for updates

Atomic-thick 2D MoS$_2$/insulator interjection structures for enhancing nanogenerator output

Xin Cui,[a] Qi Xu,[b] Xia Ni, ID *[a] Yan Zhang*[c] and Yong Qin*[ab]

Ultra-small size and large electric output are highly desirable for piezoelectric nanogenerators for powering nanodevices. However, ultra-small size usually leads to low output. Here, we simulated the output performance of MoS$_2$ nanogenerators based on atomic-thick 2D MoS$_2$/insulator interjection structures and their rational integration. We showed that the output performance is greatly increased by selecting SiO$_2$ as the insulator material, decreasing the thickness of insulator layers and increasing the side length of MoS$_2$ unit layers. When mechanically resonant with external pressure at a frequency of 215 MHz, the output generated from our rationally designed nanogenerator (70 μm × 70 μm × 5.2 μm) reaches 36 mW (corresponding to an average power density of 735 W cm^{-2}) and this output was able to directly power some nanodevices that usually need several milliwatts. Such a high power-density positions our rationally designed nanogenerator as a first-class high-efficiency nanogenerator. In addition, a significantly high instantaneous conversion efficiency of 71% from mechanical energy to electrical energy can be achieved. Our work may give some suggestions for the rational design and experimental realization of ultra-small and high-output nanogenerators.

Introduction

In today's society, small-sized electronic devices with low power consumption have gained importance in every aspect of our lives, such as wireless sensor networks, nanorobotics, and implantable biomedical nanodevices.[1–4] Because of their low volume energy density and limited lifetimes, conventional secondary batteries (*e.g.* rechargeable lithium-ion batteries) cannot supply enough power to the above-mentioned nanodevices.[5,6] To solve this problem, compact piezoelectric nanogenerators have been proposed and extensively investigated in the past decade to efficiently and continuously harvest mechanical energies from the environment to supply power without recharging procedures.[7,8] To date, the output of piezoelectric nanogenerators has been enhanced significantly and the highest power density of a single piezoelectric nanogenerator has even reached up to 17.5 mW cm^{-2} at a resistance of 200 MΩ.[9] Such a high-output nanogenerator can power a variety of devices and systems, such as commercial light-emitting diodes (LEDs),[9,10] liquid crystal displays,[11,12] and wireless data transmitters.[13] However, for some important nanodevices under certain conditions, such as implantable nanosensors,

powering them requires simultaneously small-sized and high-output power sources. Therefore, the design and subsequent fabrication of ultra-small sized and high-output nanogenerators are highly desirable, but still challenging.

The occurrence of two-dimensional (2D) materials with outstanding piezoelectric properties, such as MoS$_2$, opens up exciting possibilities for atomic-thick nanogenerators with considerable power capability.[14,15] Theoretical and experimental studies have found that monolayer MoS$_2$ possesses strong piezo-electric properties (3.78 pm V^{-1}), large mechanical stretchability (11%), and higher average breaking strength (23 GPa), which are essential for generating high-power with ultra-small size.[16,17] These properties indicate that monolayer MoS$_2$ can be a promising candidate piezoelectric material for small-sized nanogenerators with high electrical output. It has been found that for 2D MoS$_2$ layered materials, the piezoelectric output is very sensitive to the number of atomic layers.[18,19] For odd numbers of atomic layers, the piezoelectric output is large and it decreases as the number of layers increases, whereas MoS$_2$ with even numbers of layers exhibits no piezoelectric output due to its centrosymmetric structure. Therefore, to obtain a high performance 2D MoS$_2$-based nanogenerator with reduced size and large electric output, the rational design of the power unit structure and the corresponding unit integration is extremely important.

In this work, a layer-by-layer structure with MoS$_2$ monolayers and insulator layers interjected with each other was designed to considerably increase the output of the nanogenerator. In this structure, the MoS$_2$ monolayers are integrated in the same

a Institute of Nanoscience and Nanotechnology, School of Physical Science and Technology, Lanzhou University, Lanzhou 730000, China. E-mail: nix@lzu.edu.cn, qinyong@lzu.edu.cn

b School of Advanced Materials and Nanotechnology, Xidian University, Xi'an 710071, China

c School of Physical Electronics, University of Electronic Science and Technology of China, Chengdu 610054, China. E-mail: zhangyan@uestc.edu.cn

This journal is © The Royal Society of Chemistry 2018

J. Mater. Chem. C, 2018, **6**, 899–906 | 899

orientation, which maintains the advantage of the monolayer and simultaneously completely avoids piezoelectric output decay induced by the increasing atomic layers. To increase the output, the electromechanical characteristics of the tiny power generating units are evaluated and optimized. To further enhance the output and robustness of the power generating unit, a non-contact and integrated design MoS$_2$ nanogenerator based on the power generating unit is adopted. We have calculated the influence of frequency and load resistance on the voltage, current, power, and conversion efficiency of the MoS$_2$ nanogenerator. Upon simulating at a sinusoidal pressure of 1 MPa and a frequency of 215 MHz, the average output power of the small-sized MoS$_2$ nanogenerator is 36 mW and the area power density is 735 W cm^{-2}, which is larger than that of the experimental record of 17.5 mW cm^{-2} (with the peak power density at a frequency of 0.33 Hz).[9] A high instantaneous conversion efficiency of 71% for the nanogenerators is already comparable to that of the theoretical record (78%) of conventional bulk piezoelectric generators.[20] This work provides a new design to fabricate ultra-small and high-output nanogenerators.

Results and discussion

Power generating units

In order to pack MoS$_2$ monolayers within a small size and without the decrease of output, a power generating unit with the array assembly of a MoS$_2$ monolayer as shown in Fig. 1 is designed. First, a layer of insulator is placed on the MoS$_2$ monolayer, which constitutes the unit layer of the power generating unit (Fig. 1a). Then, another unit layer is superimposed on this unit layer (Fig. 1b).

Such a process is repeated until 6 unit layers are formed (Fig. 1c). Since the MoS$_2$ monolayer exhibits an in-plane piezoelectric polarization direction, the in-plane pressure is applied (Fig. 1d). The side length is 55 nm, and the thickness of the power generating unit is $n \times (0.65 + t)$ nm, where n is the number of unit layers of the power generating unit, 0.65 nm is the thickness of the MoS$_2$ monolayer,[16] and t is the thickness of the insulator layer. A pressure of 1 MPa was uniformly applied onto the top surface of the power generating unit. The base of the power generating unit is mechanically fixed and electrically grounded. The coefficients of monolayer MoS$_2$ are as follows: the elastic constants are $C_{11} = 200$ GPa and $C_{12} = 49$ GPa, the piezoelectric constant is $e_{11} = 0.56$ C m^{-2}, and the relative dielectric constant is $\varepsilon_r = 3.7$.[15,21]

The mechanical and electrical structures of the power generating unit need to be optimized to maximize the output performance. The static electrical characteristics of the power generating unit, including capacitance, charge density on the top electrode and open circuit voltage, are simulated by the COMSOL software package as used in previous studies.[22,23] The piezoelectric equation under a small uniform mechanical strain is given by:[23–25]

$$T = c_E s - e^T E \tag{1}$$

$$D = es + \kappa E \tag{2}$$

where T is the stress tensor, s is the mechanical strain, D is the electric displacement, E is the electric field, c_E is the elasticity tensor, e is the piezoelectric coefficient, and κ is the dielectric tensor.

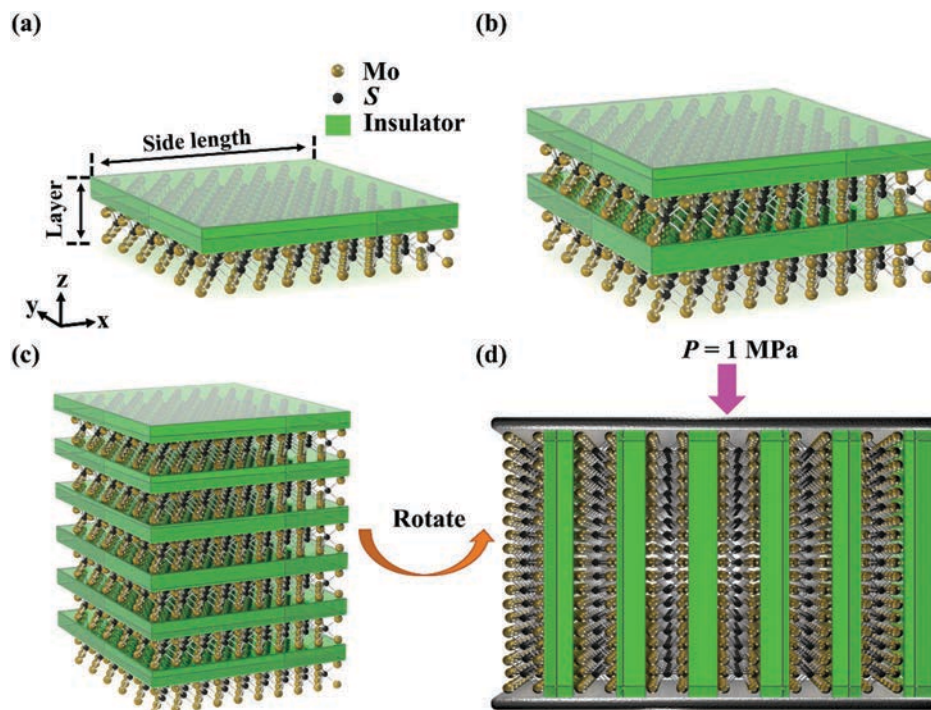In our work, four different inorganic insulating materials were adopted: SiC, Si$_3$N$_4$, Al$_2$O$_3$, and SiO$_2$, which are typically

Fig. 1 schematic diagram of the power generating unit where Mo atoms are gold, S atoms are black, and insulator layers are green.

900 | J. Mater. Chem. C, 2018, 6, 899–906

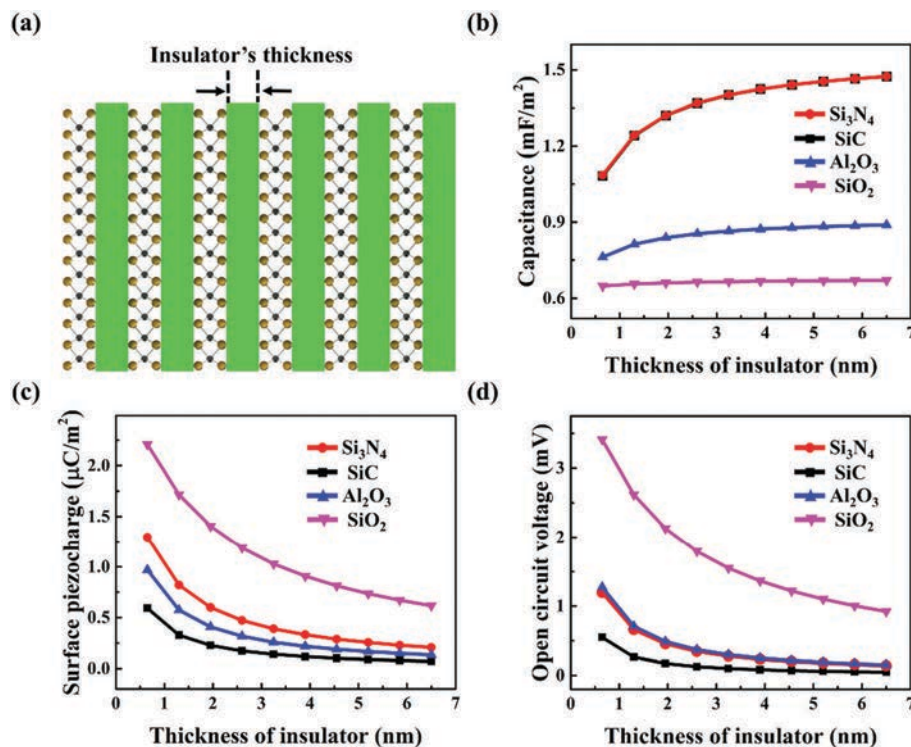This journal is © The Royal Society of Chemistry 2018

Fig. 2 Simulation of a power generating unit with different thicknesses of the insulator layer. (a) Schematics of a power generating unit with various thicknesses of the insulator. (b) Capacitance, (c) charge density on the top electrode, and (d) open circuit voltage as a function of the insulator layer thickness with different insulating materials: SiC, Si_3N_4, Al_2O_3, and SiO_2. Note that the curves of Si_3N_4 and SiC in (b) and the curves of Si_3N_4 and Al_2O_3 in (d) are overlapped.

used as insulator materials in the current semiconductor industry.[23,26] These insulating materials are easily fabricated by the current industrial technologies. Moreover, the thickness of the inorganic insulating material described above can be made to be extremely thin and can meet the demands of the power generating unit. It is clear that a polymer cannot be a suitable candidate as the insulator layer because its thickness cannot be sufficiently thin as compared to the thickness of the MoS_2 monolayer (0.65 nm).[16]

The dependences of capacitance, charge density on the top electrode, and open circuit voltage of the power generating unit on the thickness of the insulator are shown in Fig. 2. Fig. 2a shows the schematics of a power generating unit with various insulator thickness. When the thickness of the insulator layer varies from 0.65 nm to 6.5 nm, capacitance increases with thickness, as shown in Fig. 2b. The increased capacitance is due to the decreased proportion of MoS_2 in the power generating unit and the lower relative dielectric constant of MoS_2 (ε_r = 3.7) when compared with the insulators (SiC ε_r = 9.7, Si_3N_4 ε_r = 9.7, Al_2O_3 ε_r = 5.7, and SiO_2 ε_r = 4.2). Since the difference in the relative dielectric constant between MoS_2 and SiO_2 is negligible, the capacitance increases slowly as the SiO_2 insulator layer becomes thicker. Two curves of SiC and Si_3N_4 coincided because their relative dielectric constants are the same.

The compression of piezoelectric materials will generate piezoelectric polarization charges. And the charge density on the top electrode σ_p is given by $\sigma_p = d_{33}P$. Obviously, the charge

density on the top electrode is directly proportional to the piezoelectric coefficient (d_{33}) of the piezoelectric material and the pressure (P) applied on the top surface of the power generating unit.[27] When the non-piezoelectric insulator layer becomes thick and the pressure is fixed at 1 MPa, the equivalent piezoelectric constant of the power generating unit is reduced, which results in a decrease of the charge density on the top electrode as shown in Fig. 2c.

Our model is a capacitor-like plate structure, which has been generally adopted in previous studies.[11,22] According to $V_{oc} = z\sigma_p(z)/\varepsilon$, the open circuit voltage of the power generating unit is determined by the side length of the unit layer (z), charge density on the top electrode (σ_p), and the dielectric constant (ε) of the power generating unit.[25] Due to the increased capacitance and the decreased charge density on the top electrode, the open circuit voltage decreases as the thickness of the insulator layer changes from 0.65 nm to 6.5 nm, as shown in Fig. 2d. These results demonstrate that the decrease in the thickness of the insulator layer can effectively enhance the open circuit voltage.

The influences of the side length of the unit layer on the output performance are studied (Fig. 3a). As the side length of the unit layer increases from 55 nm to 100 nm, the distance between the top electrode and the bottom electrode increases, consequently leading to a decrease in capacitance (Fig. 3b). Because of the same relative dielectric constant, the two curves of SiC and Si_3N_4 are consistent. As shown in Fig. 3c, when the side length of the power generating unit is increased, the

This journal is © The Royal Society of Chemistry 2018
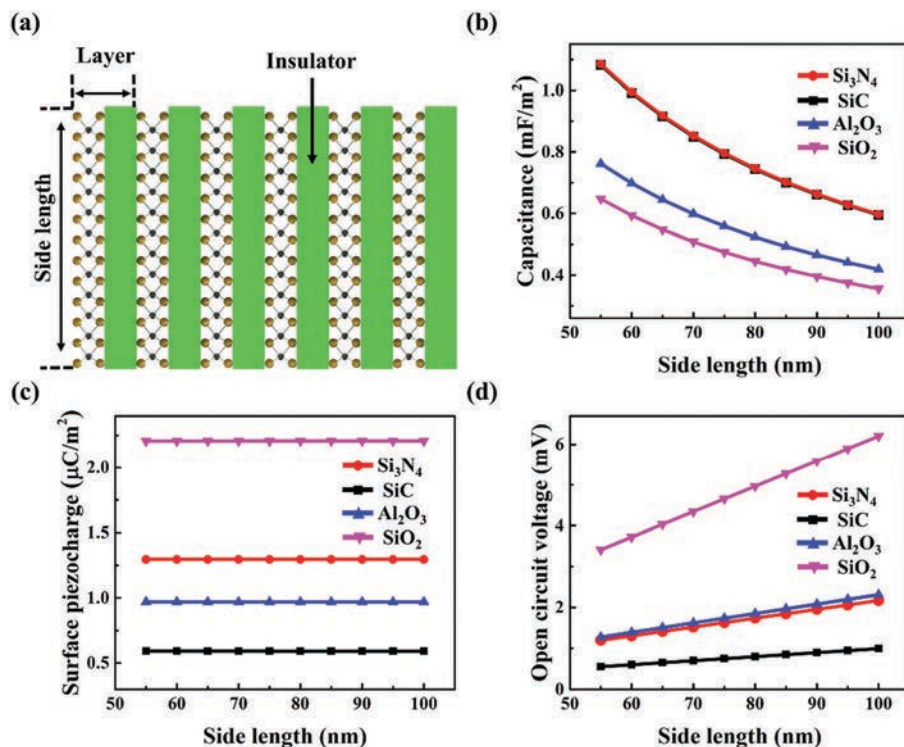
J. Mater. Chem. C, 2018, 6, 899–906 | 901

Fig. 3 The influence of the side length of the unit layer on the output of the power generating unit. (a) Schematics of the power generating unit using various side lengths of the unit layer. The effect of the side length of the unit layer on (b) capacitance, (c) charge density on the top electrode, and (d) open circuit voltage. Note that the curves of SiC and Si_3N_4 in (b) are overlapped.

charge density on the top electrode remains constant which is caused by the unchanged proportion of MoS_2 in the power generating unit. Because of the increased capacitance and the unchanged charge density on the top electrode, the open circuit voltage increases (Fig. 3d). One should mention here that, to avoid the computational convergence problems that usually occur when the length to thickness ratio is larger than 100,[14] the maximum side length of the power generating unit is set to be 100 nm, which is much smaller than the μm-level size of the experimentally prepared MoS_2 monolayer.[28] Because the open circuit voltage increases with increasing side length, we can expect that the circuit voltage can be further enhanced when the side length is increased to μm-level.

The effect of the number of layers on the static output of the power generating unit is also investigated (Fig. 4a). The capacitance depends on the proportion of MoS_2 and the distance between the top electrode and bottom electrode, and the charge density on the top electrode is determined by the proportion of MoS_2. When the MoS_2 content and electrode distance are fixed, capacitance (Fig. 4b) and charge density on the top electrode (Fig. 4c) remain unchanged. Therefore, the open circuit voltage remains unchanged (Fig. 4d). In addition, the two curves of SiC and Si_3N_4 coincide with each other due to their same relative dielectric constant. Taking into account the above results, it can be concluded that SiO_2 is an excellent candidate insulating material because of its low relative dielectric constant ($\varepsilon_r = 4.2$) and relatively low Young's modulus (70 GPa). This specific advantage will undoubtedly help to achieve the flexibility of

the nanogenerator, which is essential for powering future flexible electronic devices.

In order to achieve a higher output, in the design of a power generating unit, a thinner insulator layer, a larger side length of monolayer MoS_2, and an insulator material with a low Young's modulus and a low dielectric constant are required.

Dynamic output of integrated power generating units

The power generated by a single power generating unit is relatively low and may not be sufficient to continuously drive the nanodevice. To further enhance the output and extend the life cycle of the power generating unit, an integrated and non-contact design of the MoS_2 nanogenerator based on power generating units was adopted. The structure of the MoS_2 nanogenerator consisting of power generating units encapsulated in a polymer matrix is schematically shown in Fig. 5. First, a polymer film is used as the flexible substrate. Then, the power generating units are uniformly dispersed onto the surface of the substrate (Fig. 5a). After, another layer of polymer is "spin-coated" onto the substrate as an insulation layer to form a composite. Finally, the electrodes are "deposited" on the top and bottom surface of the composite (Fig. 5b). The simulated structure of the MoS_2 nanogenerator includes 7 × 7 power generating units with a size of 9 μm × 9 μm × 5 μm, and the size of the nanogenerator structure is 70 μm × 70 μm × 5.2 μm. As for the boundary conditions, the bottom electrode is fixed and grounded. In this study, the power generating units are considered as a piezoelectric composite material to overcome the computational

902 | *J. Mater. Chem. C*, 2018, **6**, 899–906

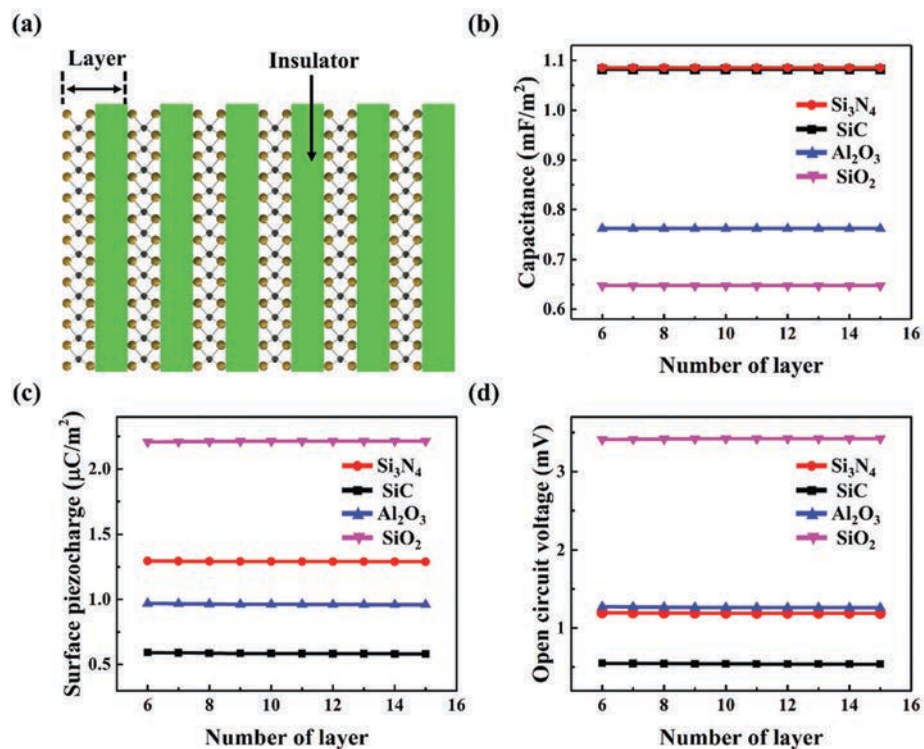This journal is © The Royal Society of Chemistry 2018

Fig. 4 Piezoelectric outputs from the power generating unit with an increased number of unit layers. (a) Schematics of a power generating unit with different numbers of unit layers. (b) Capacitance, (c) charge density on the top electrode, and (d) open circuit voltage as a function of the number of unit layers. Note that the curves of SiC and Si_3N_4 in (b) are overlapped.

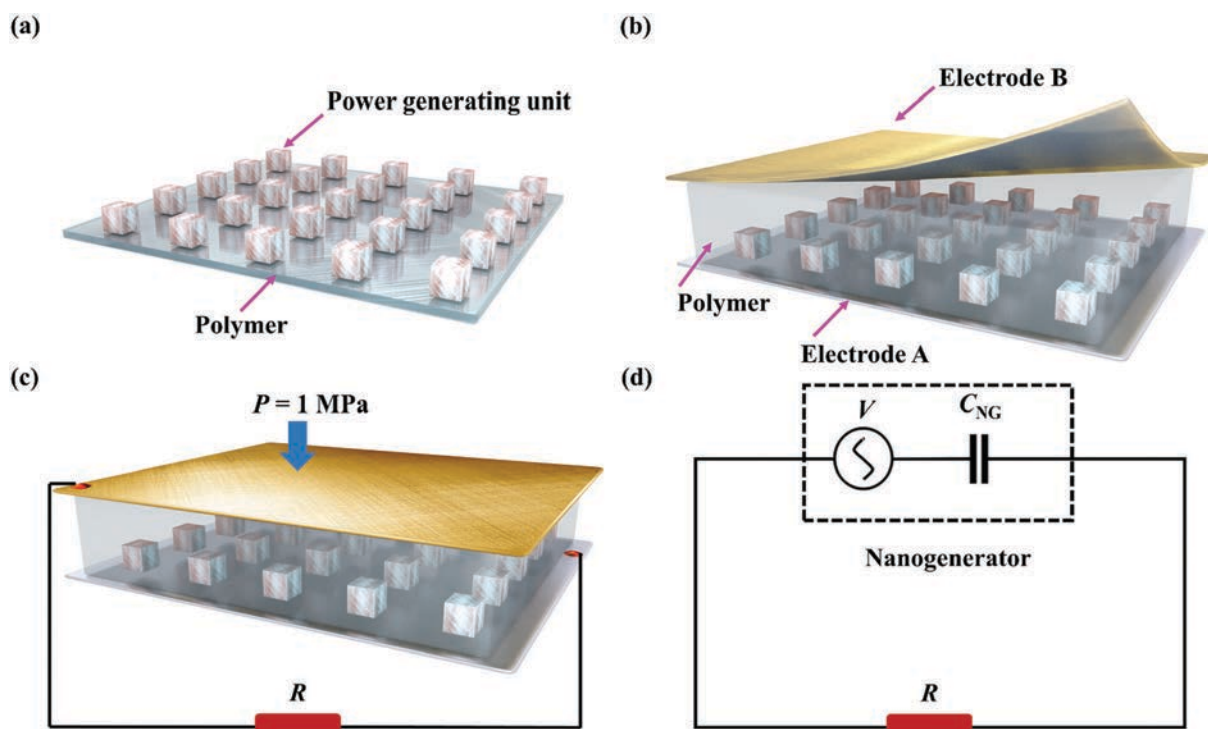Fig. 5 The structure and equivalent circuit of the MoS_2 nanogenerator. (a) Design of the MoS_2 nanogenerator. (b) A schematic diagram showing the structure of the nanogenerator. (c) A schematic illustration of a MoS_2 nanogenerator in connection with a single load resistor. (d) An equivalent circuit of the MoS_2 nanogenerator.

This journal is © The Royal Society of Chemistry 2018

J. Mater. Chem. C, 2018, 6, 899–906 | 903

convergence problems that usually occur when the length to thickness ratio of monolayer MoS_2 and the insulator layer is larger than 100.[14]

Mechanical energies collected by piezoelectric nanogenerators usually have dynamically varying vibration frequencies. Thus, it is highly desirable to study the corresponding dynamic response of these nanogenerators to these mechanical vibrations at varying frequencies, in order to continuously collect the mechanical energies and convert them into electrical energy for powering nanodevices continuously. To test the dynamic output characteristics of the MoS_2 nanogenerator in the circuit, the simulation structure is a MoS_2 nanogenerator connected to an external loaded resistor and sinusoidal pressure is applied, as shown in Fig. 5c. The equivalent circuit of the simulation model consists of a voltage source (V), a capacitor (C_{NG}), and a load resistor (R) for modeling the power consumed by the terminal load, as shown in Fig. 5d. As the MoS_2 nanogenerator has a thin thickness (5.2 μm), its capacitance is very small, which makes the MoS_2 nanogenerator more suitable for high-frequency functional devices.

Under a load resistance of 12 kΩ, the dynamic responses of the nanogenerator at different vibration frequencies are investigated. Fig. 6 shows the voltage, current, power, and conversion efficiency as a function of frequency when the nanogenerator is excited by sinusoidal pressure. For the two different types of matrix polymer materials, the first order resonance frequency of the nanogenerator is calculated to be 215 MHz for polymethylmethacrylate (PMMA) and 290 MHz for polydimethylsiloxane (PDMS). The simulation results show that

the maximum voltage reached was 24.6 V (Fig. 6a) and the maximum current was 2 mA (Fig. 6b) for the nanogenerator packaged with PMMA. The maximum voltage and current were 10.9 V and 0.9 mA, respectively, for the nanogenerator packaged with PDMS. This indicates that the performance of the nanogenerator can be significantly improved when packaged with PMMA. The dependence of power and conversion efficiency on mechanical vibration frequency shown in Fig. 6c and d further proves that the nanogenerator works most effectively at the resonance frequency. The resonance frequency of the nanogenerator is represented by the following equation:[29]

$$f = \frac{3.52}{2\pi L^2}\sqrt{\frac{EI}{\rho A}} \qquad (3)$$

where E is the Young's modulus of the nanogenerator material, I is the geometrical moment of inertia, A is the cross-sectional area, r is the mass density per unit volume, and L is the length of the nanogenerator. By changing the parameters of the materials and the geometrical shape of the nanogenerator, the resonance frequency can be controlled arbitrarily and the nanogenerator can harvest mechanical energy efficiently over a wide frequency range.

Finally, the output of the nanogenerator packaged with PMMA under different load resistances is studied (Fig. 7). Fig. 7a shows the voltage and current outputs as a function of load resistance at the resonance frequency of 215 MHz. The voltage first increases with the load resistance and reaches its maximum value near
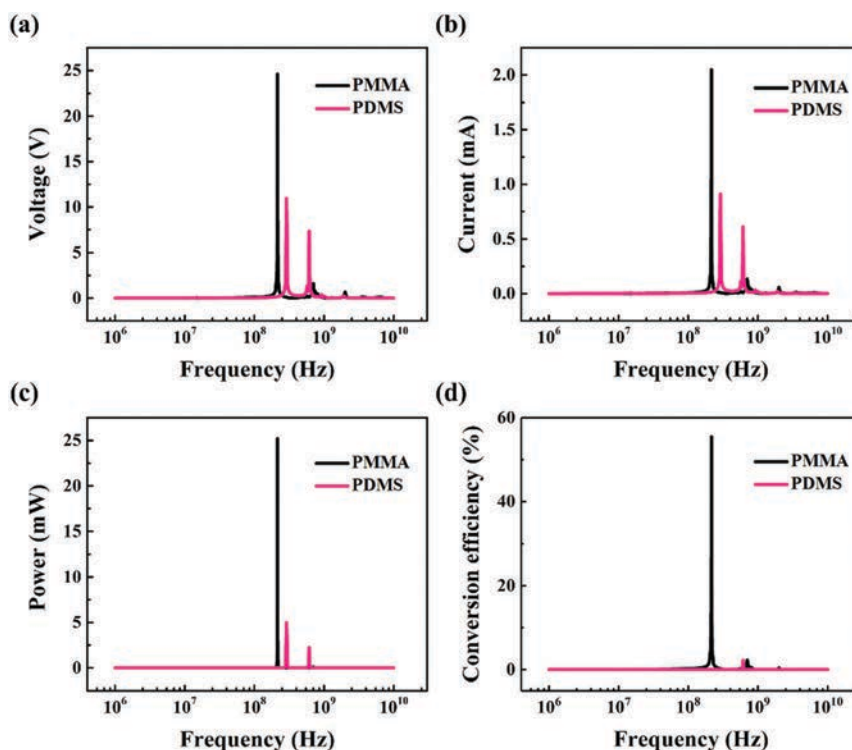

Fig. 6 Frequency dependence of the MoS_2 nanogenerator output under a load resistance of 12 kΩ. (a) Voltage, (b) current, (c) power, and (d) conversion efficiency depending on the excitation frequency.
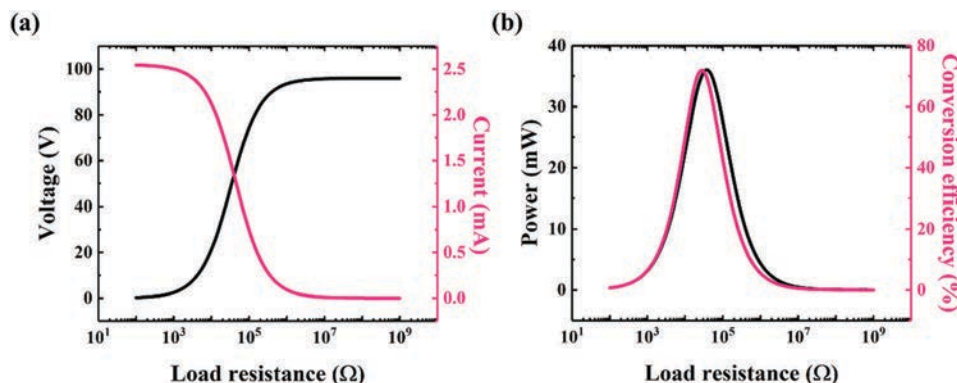
904 | *J. Mater. Chem. C,* 2018, **6**, 899–906

This journal is © The Royal Society of Chemistry 2018

Fig. 7 Resistance dependence of the MoS$_2$ nanogenerator outputs. (a) Voltage and current of a MoS$_2$ nanogenerator as a function of load resistance. (b) The effects of load resistance on power and conversion efficiency.

10 MΩ, whereas the current output decreases with the load resistance until 10 MΩ and then tends to remain unchanged. In Fig. 7b, it can be seen that the maximum power of 36 mW (power densities of 735 W cm^{-2} and 1.41 MW cm^{-3}) is achieved for a load resistance of 40 kΩ under a sinusoidal pressure of 1 MPa and a frequency of 215 MHz. It is worth emphasizing that the power of the MoS$_2$ nanogenerator can be further enhanced by increasing the applied pressure because the pressure exerted on the nanogenerator (1 MPa) is far below the average breaking strength of monolayer MoS$_2$ of 23 GPa.[16] Simulation results also show that the maximum conversion efficiency was 71% ($\eta = W_E/W_M$) when a load resistance of 25 kΩ was applied, which was determined by the electromechanical characteristics and the vibration frequency of the nanogenerator according to previous research.[30]

Conclusions

In the present work, we have designed a small-sized and high-output MoS$_2$ nanogenerator. By the layer-by-layer assembly of MoS$_2$ monolayers and insulator layers, MoS$_2$ monolayers were integrated into a small-sized power generating unit. Upon decreasing the thickness of the insulator layer and increasing the side length of the unit layer, the output voltage is increased. A maximum power of 36 mW (power densities of 735 W cm^{-2} and 1.41 MW cm^{-3}) and an instantaneous conversion efficiency of 71% have been achieved by a nanogenerator with integrated power generating units. Our design provides some suggestions for the rational design and experimental realization of ultra-small and high output nanogenerators.

Conflicts of interest

The authors declare no competing financial interests.

Acknowledgements

References

1 F. R. Fan, W. Tang and Z. L. Wang, *Adv. Mater.*, 2016, **28**, 4283–4305.
2 Y. Hu and Z. L. Wang, *Nano Energy*, 2015, **14**, 3–14.
3 Z. L. Wang and W. Wu, *Angew. Chem., Int. Ed.*, 2012, **51**, 11700–11721.
4 Z. L. Wang, J. Chen and L. Lin, *Energy Environ. Sci.*, 2015, **8**, 2250–2282.
5 N. S. Lewis, *Science*, 2007, **315**, 798–801.
6 Y. Zi, H. Guo, Z. Wen, M. H. Yeh, C. Hu and Z. L. Wang, *ACS Nano*, 2016, **10**, 4797–4805.
7 J. Chun, N.-R. Kang, J.-Y. Kim, M.-S. Noh, C.-Y. Kang, D. Choi, S.-W. Kim, Z. L. Wang and J. Min Baik, *Nano Energy*, 2015, **11**, 1–10.
8 Z. L. Wang and J. Song, *Science*, 2006, **312**, 242–246.
9 K. I. Park, J. H. Son, G. T. Hwang, C. K. Jeong, J. Ryu, M. Koo, I. Choi, S. H. Lee, M. Byun, Z. L. Wang and K. J. Lee, *Adv. Mater.*, 2014, **26**, 2514–2520.
10 L. Gu, N. Cui, L. Cheng, Q. Xu, S. Bai, M. Yuan, W. Wu, J. Liu, Y. Zhao, F. Ma, Y. Qin and Z. L. Wang, *Nano Lett.*, 2013, **13**, 91–94.
11 Y. Hu, Y. Zhang, C. Xu, G. Zhu and Z. L. Wang, *Nano Lett.*, 2010, **10**, 5025–5031.
12 W. Wu, S. Bai, M. Yuan, Y. Qin, Z. L. Wang and T. Jing, *ACS Nano*, 2012, **6**, 6231–6235.
13 Y. Hu, Y. Zhang, C. Xu, L. Lin, R. L. Snyder and Z. L. Wang, *Nano Lett.*, 2011, **11**, 2572–2577.
14 Y. Zhou, W. Liu, X. Huang, A. Zhang, Y. Zhang and Z. L. Wang, *Nano Res.*, 2016, **9**, 800–807.
15 K.-A. N. Duerloo, M. T. Ong and E. J. Reed, *J. Phys. Chem. Lett.*, 2012, **3**, 2871–2876.
16 S. Bertolazzi, J. Brivio and A. Kis, *ACS Nano*, 2011, **5**, 9703–9709.
17 S. K. Kim, R. Bhatia, T.-H. Kim, D. Seol, J. H. Kim, H. Kim, W. Seung, Y. Kim, Y. H. Lee and S.-W. Kim, *Nano Energy*, 2016, **22**, 483–489.
18 W. Wu, L. Wang, Y. Li, F. Zhang, L. Lin, S. Niu, D. Chenet, X. Zhang, Y. Hao, T. F. Heinz, J. Hone and Z. L. Wang, *Nature*, 2014, **514**, 470–474.

19 H. Zhu, Y. Wang, J. Xiao, M. Liu, S. Xiong, Z. J. Wong, Z. Ye, Y. Ye, X. Yin and X. Zhang, *Nat. Nanotechnol.*, 2015, **10**, 151–155.

20 T. Funasaka, M. Furuhata, Y. Hashimoto and K. Nakamura, *Proc. - IEEE Ultrason. Symp.*, 1998, **1**, 959–962.

21 D. Davelou, G. Kopidakis, G. Kioseoglou and I. N. Remediakis, *Solid State Commun.*, 2014, **192**, 42–46.

22 X. Huang, L. Li and Y. Zhang, *Sci. China: Technol. Sci.*, 2013, **56**, 2622–2629.

23 R. Hinchet, S. Lee, G. Ardila, L. Montès, M. Mouis and Z. L. Wang, *Adv. Funct. Mater.*, 2014, **24**, 971–977.

24 Y. Gao and Z. L. Wang, *Nano Lett.*, 2007, **7**, 2499–2505.

25 Z. L. Wang, *Mater. Today*, 2017, **20**, 74–82.

26 H. Morkoç, S. Strite, G. B. Gao, M. E. Lin, B. Sverdlov and M. Burns, *J. Appl. Phys.*, 1994, **76**, 1363–1398.

27 A. Qaiss, H. Saidi, O. Fassi-Fehri and M. Bousmina, *Polym. Eng. Sci.*, 2013, **53**, 105–111.

28 Z. Tu, G. Li, X. Ni, L. Meng, S. Bai, X. Chen, J. Lou and Y. Qin, *Appl. Phys. Lett.*, 2016, **109**, 223101.

29 A. Yu, P. Jiang and Z. L. Wang, *Nano Energy*, 2012, **1**, 418–423.

30 E. Lefeuvre, D. Audigier, C. Richard and D. Guyomar, *IEEE Trans. Power Electron.*, 2007, **22**, 2018–2025.